



## Importance of bridge-specific fragility curves in the seismic assessment of road networks

A.J. Kappos<sup>(1)</sup>, S.P. Stefanidou<sup>(2)</sup>

<sup>(1)</sup> Department of Civil Engineering, City University London, Professor, [Andreas.Kappos.1@city.ac.uk](mailto:Andreas.Kappos.1@city.ac.uk)

<sup>(2)</sup> Department of Civil Engineering, Aristotle University of Thessaloniki, Postdoctoral Researcher, [ssotiria@civil.auth.gr](mailto:ssotiria@civil.auth.gr)

### **Abstract**

In general, bridges within a road network have different geometries, structural systems and member properties, mainly due to differences in the site topography and the construction method selected; therefore, the use of the same seismic fragility functions for all bridges of a certain class, neglecting the specific characteristics of their key components and of the seismic demand (that also varies with the site) is in principle inconsistent, albeit commonly done in loss assessment projects. To gain more insight into this, this paper focuses on the application of a recently proposed methodology for the derivation of bridge-specific fragility curves to all different bridge categories within an actual road network, hence revealing the importance of the bridge-specific approach in assessing a bridge inventory. Capacity and demand are explicitly defined at a component level for all different bridges and bridge categories of the studied road network, using advanced analysis tools (ad-hoc developed software), while uncertainties in capacity, demand and limit state definition are accounted for, based on the results of inelastic pushover and response history analyses. Using this approach, fragility curves for different limit states are derived at both the component and system level, for all bridges of the road network studied, while the consistency of adopting ‘representative’ fragility curves for all bridges belonging to the same category is also investigated. To this purpose, fragility curves for all bridges of two specific categories are presented, hence identifying the range within which the damage thresholds vary for a given typological class, whereas the effect of different geometric properties and bridge class on seismic fragility is also investigated.

*Keywords: Bridges; seismic assessment; fragility curves; road network; reinforced concrete*

## 1. Introduction

Damage due to earthquake is commonly related to substantial direct and indirect losses, highlighting the need for damage detection and retrofit prioritization based on the results of the seismic risk assessment of the road network. In this context, numerous methodologies have been developed for the seismic vulnerability assessment of bridges for different levels of seismic hazard using fragility curves; analytical [1, 2, 3] as well as empirical [4] procedures have been put forward.

Bridges in a road network have in general different structural and geometric properties depending on the site topography, the selected structural system and construction method, and the foundation soil. In the literature [1, 3, 5, 6, 7] bridges are classified into different categories, while, under the assumption that the seismic performance of bridges within the same class is similar, fragility curves of the representative -of each category- bridge are typically used for the seismic assessment of the bridge stock. The number of spans, number of columns (single or multicolumn bents), skewness, deck type, pier type and the pier-to-deck connection, are some of the parameters considered in classification schemes available in the literature [1, 3, 5, 6]. The effect of geometry (i.e. total deck length and width, pier height) on bridge fragility is fully recognized [1], [8], therefore different bridge geometries within the same category were studied in order to highlight the differences compared to the representative bridge [8, 2].

It is clear that the estimation of bridge-specific fragility curves is a rather demanding procedure since the seismic performance of critical bridge components is related to the individual bridge structural system configuration. The accuracy and consistency of the assumption that fragility curves of a ‘generic’ bridge can be used for all bridges that fall within the same category is dependent on the classification scheme adopted, however it is underlined that both component demand and capacity vary and are related to component properties. Parametric vulnerability curves are proposed in [2], introducing generic fragility functions based on analysis results of bridges having different geometries and overstrength ratios. This approach is rather appealing, however oversimplified, since neither the effect of different component properties on seismic demand and capacity, nor the effect of different structural configuration on systems’ fragility were investigated.

In the context of the above, the main objective of this paper is to apply a recently proposed (by the authors) methodology [9] for the estimation of bridge-specific fragility curves of an actual road network. Capacity is explicitly defined at component level for every individual bridge, considering the effect of different component properties on limit state thresholds, whereas component demand is also calculated at component level, based on the results of response spectrum analysis of a simplified bridge-specific 3D structural model. Using the ad-hoc developed software and the proposed methodology, bridge-specific fragility curves for the longitudinal and transverse direction are derived based on bridge-specific analysis results without considerable increase in the computational cost. It should be noted that uncertainties in capacity, limit state definition and demand are additionally accounted for on the basis of the results of inelastic pushover and response history analyses. Using this approach, bridge fragility curves for all different limit states and all bridges in the network studied are derived (considering the effect of multiple critical bridge components), while the consistency of adopting generic fragility curves for bridges that fall within the same category is also investigated. Finally, fragility curves for all representative bridges of the different bridge classes are presented with a view to highlighting the effect of different pier, deck and pier-to-deck connection types on bridge fragility, whereas the effect of bridge geometry, namely total bridge length and maximum pier height, is additionally investigated, based on limit state thresholds for all bridges and bridge classes within the network.

## 2. Methodology

The component-based methodology for the derivation of bridge-specific fragility curves for a concrete bridge stock using an ad-hoc developed software is described in detail in [9]. The main aspects of the proposed methodology are the case-specific definition of component capacity and threshold limit state values for the quantification of damage considering the effect of different component properties, failure modes and boundary conditions, as well as the elastic analysis of a simplified model for the estimation of demand at component level, and, finally, the uncertainty treatment.

Bridge piers, abutments and bearings (Fig. 1) are considered as the critical components for the system's seismic performance. Therefore, capacity is defined at component level, accounting for the effect of different geometric, material, loading and member detailing parameters on component strength and ductility and, eventually, damage threshold value.

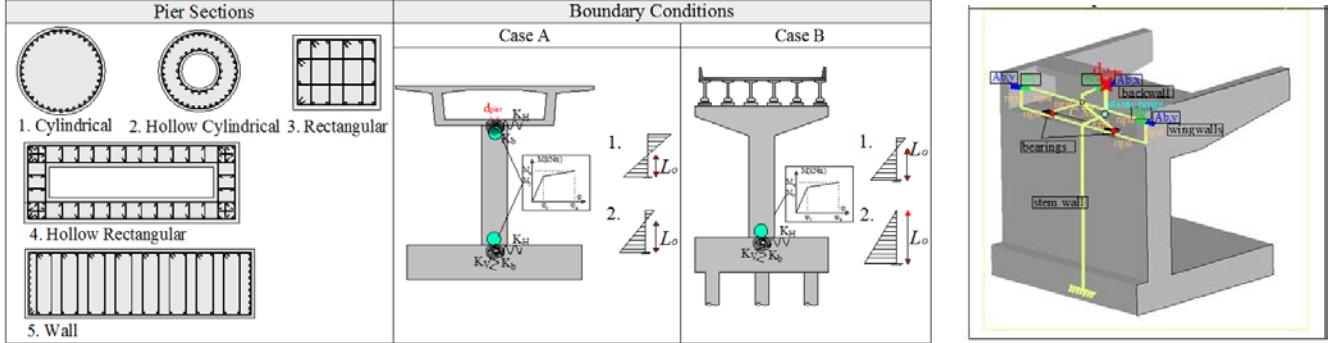


Fig. 1 – Critical bridge components - Pier types considered in the database and different boundary conditions

As described in [9], global engineering demand parameters (EDPs) are used for the quantification of component damage, accounting for different failure modes and boundary conditions. However, local to global demand parameter mapping is performed in order to describe global damage in qualitative terms. On the basis of the above, limit state (damage) thresholds for the various limit states considered in fragility analysis are defined for each critical component in terms of the displacement of the control point, as shown in Table 1.

Table 1 – Limit state thresholds for critical structural components

Limit State	R/C Piers / EDP : $d$ (m)		Abutments EDP: $d$ (m)	Bearings EDP: $\gamma$ (%)
	Local	Global		
LS 1 – Minor/Slight damage	$\varphi_1: \varphi_y$	$d_1: \min \begin{cases} d(\varphi_1) \\ d(V_1) \end{cases}$	$d_1 = 1.1 \cdot d_{gap}$ ( $\mu_{\varphi, backwall} = 1.5$ )	20 ( $d_1 = 0.02 \cdot h_{br}$ )
LS 2 – Moderate damage	$\varphi_2: \min (\varphi: \varepsilon_c > 0.004 ,$ $\varphi: \varepsilon_s \geq 0.015)$	$d_2: \min \begin{cases} d(\varphi_2) \\ d(V_2) \end{cases}$	$d_2 = 0.01 \cdot h_{backwall}$	100 ( $d_2 = 0.1 \cdot h_{br}$ )
LS 3 – Major/Extensive damage	$\varepsilon_c \leq 0.004 +$ $\varphi_3: \min (\varphi:$ $1.4 \cdot \rho_w \cdot \frac{f_{yw}}{f_{cc}}$ $\varphi: \varepsilon_s \geq 0.06)$	$d_3: \min \begin{cases} d(\varphi_3) \\ d(V_3) \end{cases}$	$d_3 = 0.035 \cdot h_{backwall}$	200 ( $d_3 = 0.2 \cdot h_{br}$ )
LS 4 – Failure/Collapse	$\varphi_4: \min (\varphi:$ $M < 0.90 \cdot M_{max} ,$ $\varepsilon_s \geq 0.075)$	$\varphi: d_4: \min \begin{cases} d(\varphi_4) \\ d(V_4) \end{cases}$	$d_4 = 0.1 \cdot h_{backwall}$	300 ( $d_4 = 0.3 \cdot h_{br}$ )

For bridge piers, damage is initially defined at section level, using local demand parameters (section curvature), related to experimentally estimated damage (e.g. crack widths). Subsequently, threshold limit state values are expressed at component level in terms of a global demand parameter, namely displacement of the control point, using a closed-form relationship proposed in [9]. The latter was derived on the basis of regression of results from pushover analysis of the reinforced concrete (R/C) piers, considering different possible failure modes (flexure and shear) as depicted in Fig. 2-b, whereas different boundary conditions (connection of the pier to the deck and the foundation) are additionally accounted for, relating the displacement of the contraflexure point (tip of equivalent cantilever) to that at the top of the restrained pier as described in Fig. 2-a and in [10].

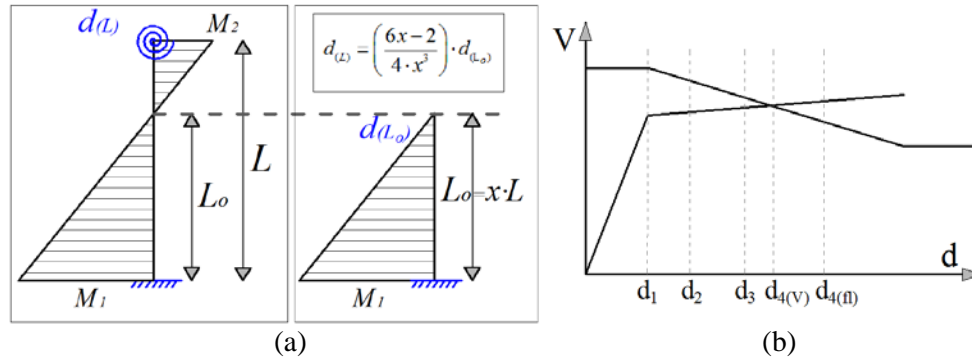


Fig. 2 – (a) Top displacement of the restrained pier correlated to displacement of contraflexure point, (b) Limit state threshold on pushover curve considering both flexural and shear failure mode

The empirical relationship used for the estimation of limit state thresholds has the form of Eq. (1). Parameters  $\alpha_{1-6}$  are defined on the basis of regression analysis and depend on pier section types (a database was set up for different section types, namely cylindrical, rectangular, hollow, etc., see Fig.1). Use of the proposed relationships ensures that the effects of different section types, as well as geometric, material, loading and reinforcement parameters on component capacity and threshold limit state values are accounted for. Threshold values calculated using Eq. (1) refer to the equivalent cantilever ( $L_o$  in Fig. 2); the level of the contraflexure point should be defined (pier top to bottom moment ratio) in order to relate them to threshold values of the restrained pier, as described in Fig. 2 and in more detail in [10].

$$\delta_1 \sim \delta_4 = \exp[\alpha_1 + \alpha_2 \cdot \ln(D/H) + \alpha_3 \cdot \ln(v) + \alpha_4 \cdot \ln(f_c/f_y) + \alpha_5 \cdot \ln(\rho_w) + \alpha_6 \cdot \ln(\rho_l)] \cdot L \quad (1)$$

For the quantification of abutment and bearing damage, threshold limit state values are defined in terms of displacement of the component control point, based on experimental results and other information from the literature, as described in [9]. In particular, threshold displacement values for abutments are related to the gap size and backwall height, while threshold displacement values for elastomeric bearings are related to shear strain (Table 1).

Component capacity and limit state thresholds are defined accounting for the bridge-specific parameters and properties; moreover, uncertainty in capacity ( $\beta_c$ ) and limit state definition ( $\beta_{LS}$ ) should also be considered; the latter depend on component type and the selected demand parameter, and are quantified in [9] and [10].

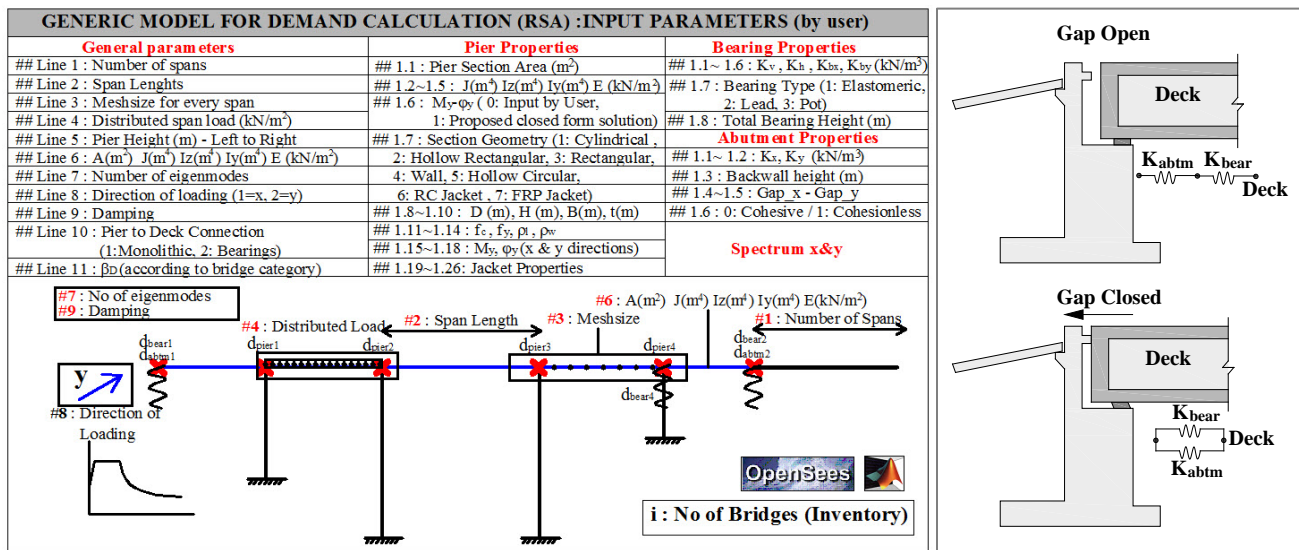


Fig. 3 – Ad-hoc software for bridge-specific fragility curves (input data – cases of open/closed gap)

The Matlab-based software developed for the implementation of the previously described methodology and the derivation of bridge-specific fragility curves is illustrated in Fig. 3. The software is based on a generic simplified 3d bridge model created using the OpenSees platform [11]. Input data provided by the user are

depicted in Fig. 3 and concern general bridge geometry and loading properties, component (pier, bearing, abutment) properties, and the (site-specific) response spectrum. Threshold limit state values for piers are automatically calculated in displacement terms according to the geometric, material, reinforcement, loading properties and boundary conditions in each case, while dispersion values, calculated in line with the procedure described in [9], are also included. Seismic demand is calculated at component level based on response spectrum analysis results for various IM levels (0.1~1.0g), while the evolution of damage with earthquake intensity is plotted for every component considered. Different boundary conditions at abutments are considered for the case of open and closed gap, whereas fragility curves are automatically calculated for longitudinal and transverse directions separately, under the assumption of series connection between components (lower bound).

The methodology described in brief above can be easily applied to all bridges in a road network using the ad-hoc developed software and is outlined in the flowchart of Fig.4.

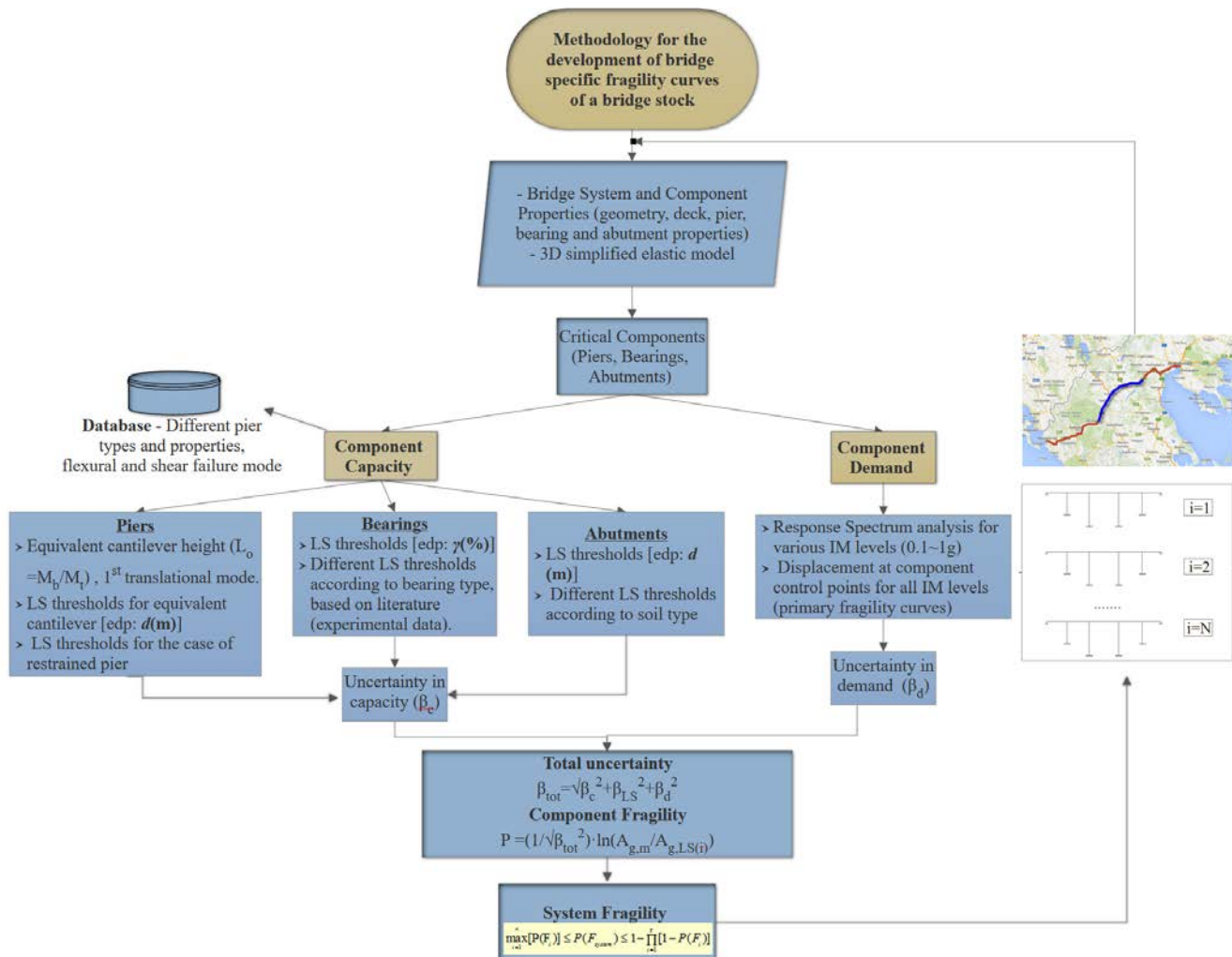


Fig. 4 – Flowchart for the component-based methodology for the derivation of bridge-specific fragility curves applied to a road network

### 3. Bridge-specific fragility curves for bridges of an existing road network

The methodology described in §2 is applied to all bridges of an Egnatia Motorway section (Western Macedonia, Greece), a total of 44. Bridge-specific fragility curves are calculated for each bridge (for the longitudinal and transverse direction separately) and the results are discussed in detail below in the context of highlighting the effect of the classification scheme adopted, as well as different geometric and material properties on bridge fragility. Furthermore, the range within which the damage thresholds vary for a given typological bridge class is

additionally investigated, highlighting the importance of the bridge-specific approach in assessing a bridge inventory.

### 3.1 Classification of Egnatia Motorway bridges

The bridges of the inventory are initially classified into categories according to the classification scheme presented in [3] and summarised in Table 2. A code number is defined for each bridge according to the pier, deck and the pier-to-deck connection type. It should be noted that the classification of bridges is not necessary for the application of the methodology proposed and the derivation of bridge-specific fragility curves. However, for reasons of practicality of the loss assessment procedure, bridges that fall within the same category can be assumed to have the same uncertainty in demand values (quantification of uncertainty is time consuming); hence the classification of bridges is used for estimation of uncertainty in seismic demand values. It is noted that the scheme is tailored to the typologies common in medium and high seismicity areas of Europe.

Table 2 – Classification scheme for bridges in a road network

X1		X2		X3	
Pier Type		Deck type		Pier-to-deck connection	
Code Number	Description	Code Number	Description	Code Number	Description
1	Single column - Cylindrical section	1	Slab (solid or with voids)	1	Monolithic
2	Single column - Hollow section	2	Box girder	2	Through bearings
3	Multi-column bent	3	Simply supported precast-prestressed beams	3	Combination of monolithic and bearing connections
4	Wall-type				
5	V-type				

All different bridge classes of the studied section of Egnatia Motorway are presented in Fig.5. Prestressed concrete box-girder bridges with hollow rectangular piers monolithically connected to the deck, constructed using the cantilever method, is the most frequent typology (25%) due to the site topography (mountainous area). Simply supported bridges where the prestressed concrete beam deck is supported on hollow rectangular piers through elastomeric bearings are the second most frequent class in the inventory, while single span and box-girder bridges with cylindrical single-column or multi-column piers monolithically connected to the deck are also frequently encountered in this inventory.

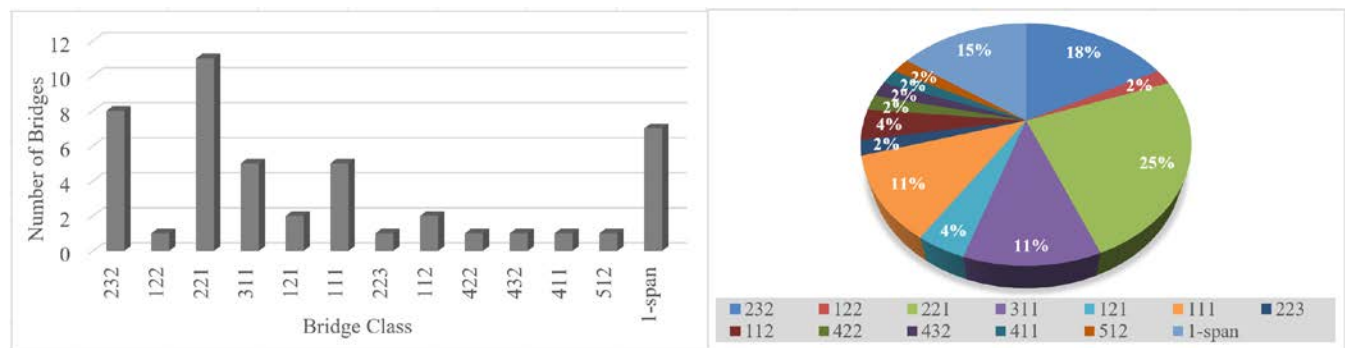


Fig. 5 – Different bridge classes in Egnatia Motorway, Western Macedonia section

### 3.2 Bridge-specific fragility curves for all bridge classes

The methodology described in §2 is applied to all bridges of the bridge stock, to derive structure-specific fragility curves. The effect of different pier, deck, pier-to-deck connection type and eventually the classification scheme selected on bridge fragility is depicted in Figures 6 to 10. The fact that these figures depict system

fragility, calculated under the assumption of series connection between components, should also be taken into account when interpreting the results.

Bridge fragility curves of the generic bridges of typological classes #111, #311, #411, namely bridges with single-column cylindrical, multi-column cylindrical and wall type piers, respectively, monolithically connected to the slab-type deck are depicted in Fig.6. The effect of different pier type on system fragility for the longitudinal and transverse direction of bridges having the same deck type and pier-to-deck connection is clear; bridges with single column piers are more vulnerable, whereas bridges with multi-column cylindrical and wall-type piers are less vulnerable. The most critical components in the case of monolithic pier-to-deck connection are bridge piers and abutments, therefore the relatively higher vulnerability in the transverse direction is due to the pier cantilever action (higher seismic demand). The use of multi-column bents results in lower seismic demand for each pier and, eventually, lower vulnerability, whereas wall-type piers have higher flexure and shear capacity (but higher seismic demand as well) compared to cylindrical single-column piers. It should be further pointed out that bridges with multi-column piers monolithically connected to the slab of the deck are less vulnerable in the longitudinal direction than bridges having the same deck, pier-to-deck connection type and wall-type piers, whereas this is not the case for the transverse direction (strong axis of wall-type pier).

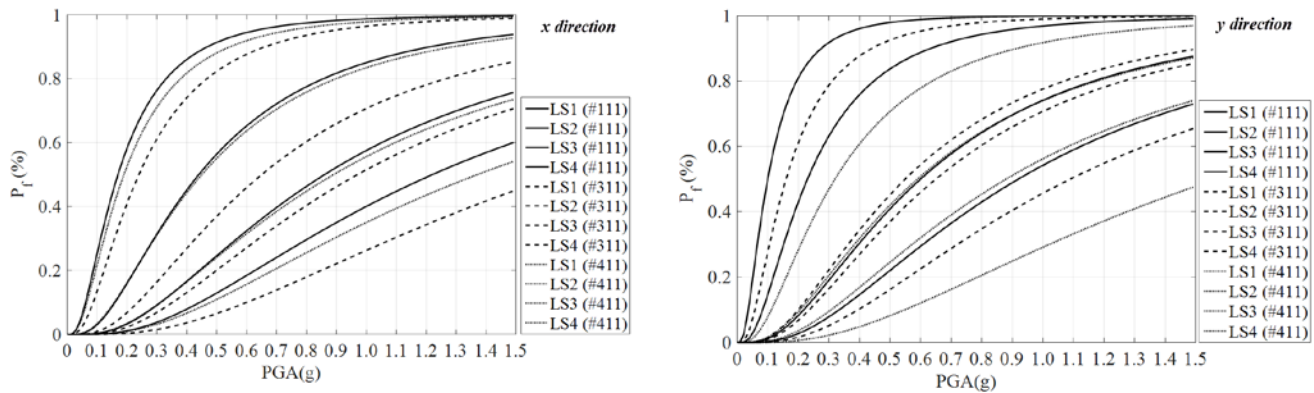


Fig. 6 – Fragility curves for the longitudinal (x) and transverse (y) direction of bridge classes #111, #311, #411

Comparing bridges with single-column cylindrical and hollow rectangular pier sections monolithically connected to the box-girder deck (classes #121 and #221, Fig. 7), the main conclusion is that bridges with hollow rectangular piers are less vulnerable, whereas the differences may become significant for the transverse direction and the higher limit states. Piers and abutments are the most critical components for the bridge classes considered. The differences are higher for LS1 and the longitudinal direction, since yielding of cylindrical piers occurs sooner, whereas the minor differences for the longitudinal direction and LS3 and LS4 are attributed to the critical component for the specific limit state (abutments). The differences in transverse direction and LS3 and LS4 should be interpreted considering pier geometry and orientation of hollow rectangular pier in the transverse direction (strong axis).

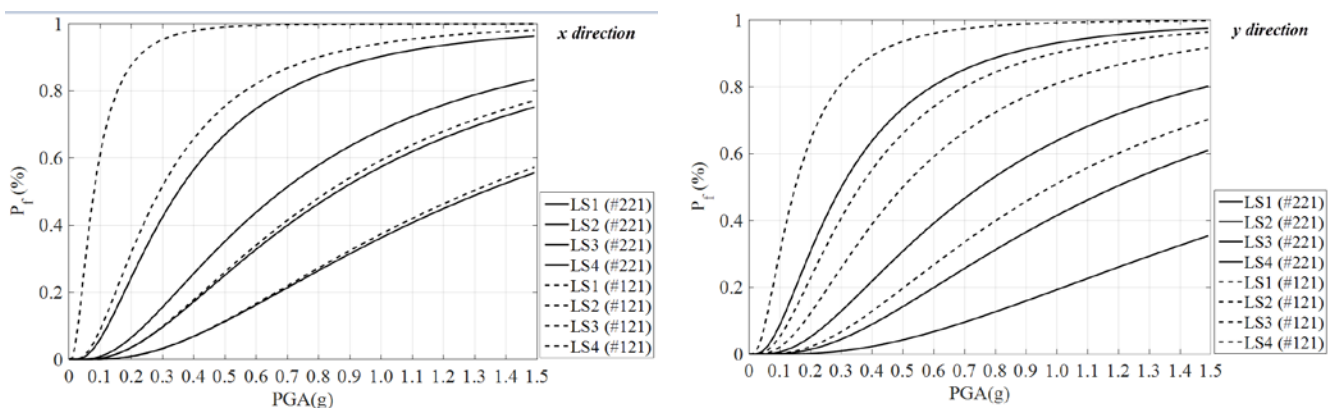


Fig. 7 – Fragility curves for the longitudinal and transverse direction of bridge classes #221, #121

The differences in system fragility for the case of simply-supported bridges having hollow rectangular or wall-type piers connected through elastomeric bearings to the prestressed concrete beam deck (categories #232 and #432, Fig.8) are low, mainly for the longitudinal, but for the transverse direction as well. The main reason is that in this case bearings are the most critical component for the majority of limit states considered.

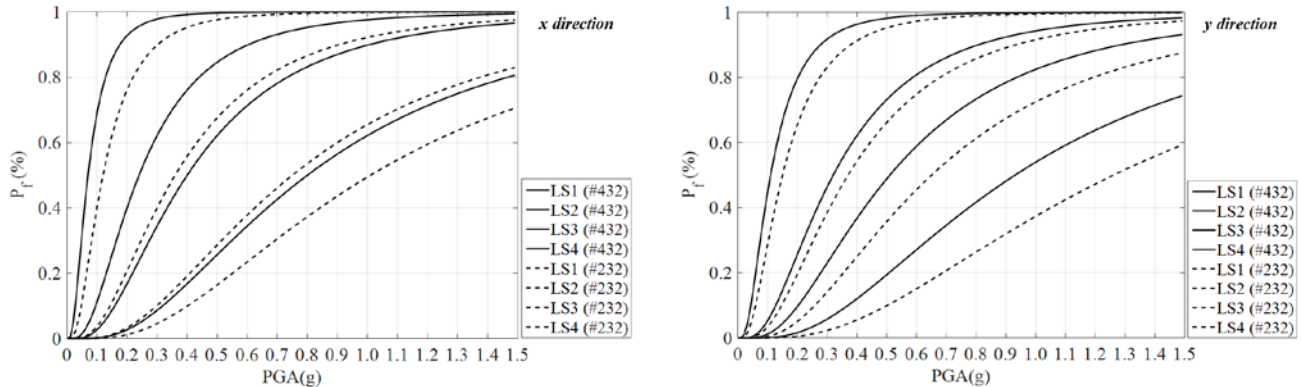


Fig. 8 – Fragility curves for the longitudinal and transverse direction of bridge classes #432, #232

The effect of different deck type, namely slab or box girder, on bridge fragility of bridges having single column cylindrical piers connected to deck through elastomeric bearings (classes #122 and #112), is in general minor, as shown in Fig.9. It should be, however, noted that the effect is higher for the longitudinal direction.

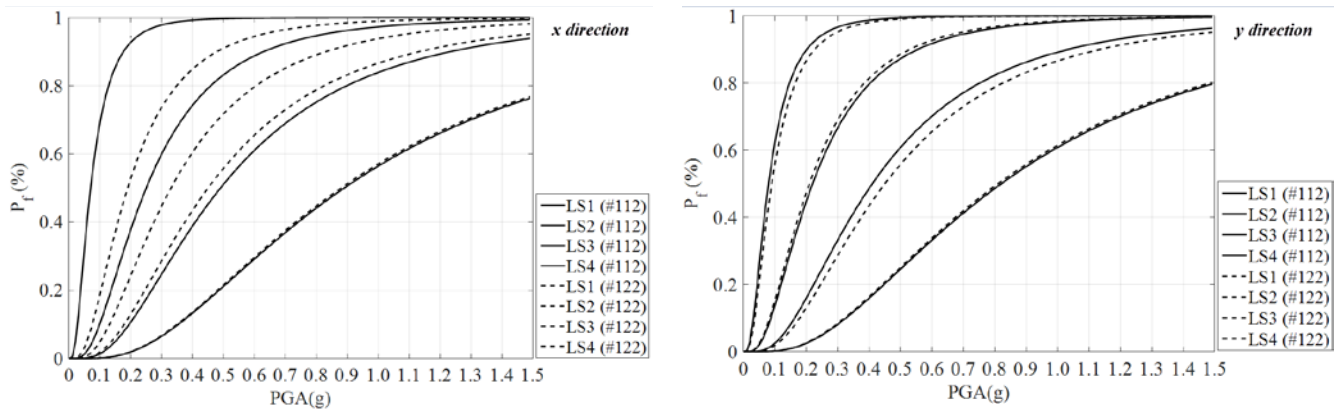


Fig. 9 – Fragility curves for the longitudinal and transverse direction of bridge classes #112, #122

Finally, the effect of pier-to-deck connection (monolithic or through elastomeric bearings) on bridges having single-column cylindrical piers and slab-type deck, is depicted in Fig.10 (categories #112 and #111). It is seen that fragility of monolithic bridges is lower for all limit states and in both the longitudinal and transverse direction. The latter is due to the fact that different components, namely bearings and piers, are critical for the seismic performance of each bridge category, mainly in the longitudinal direction.

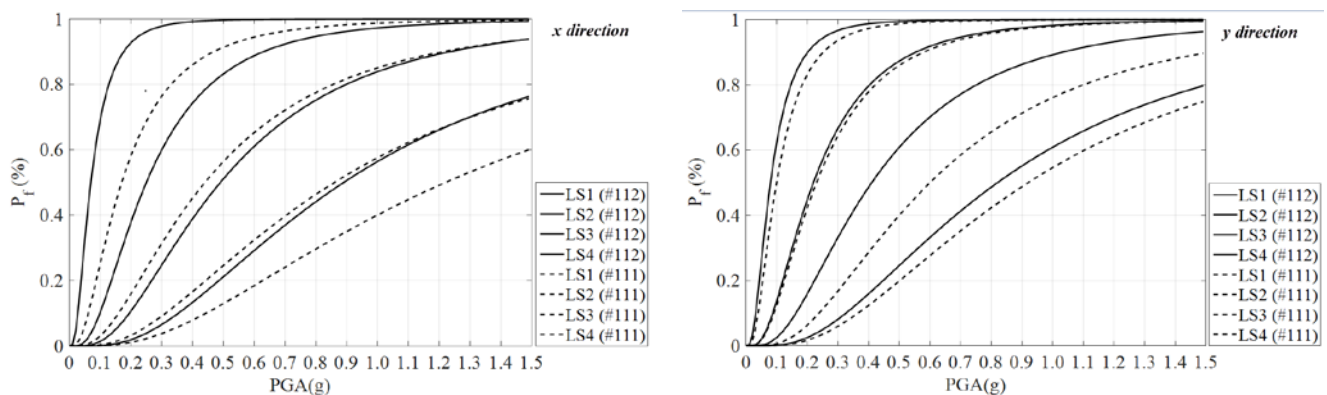


Fig. 10 – Fragility curves for the longitudinal and transverse direction of bridge classes #112, #111

### 3.3 Seismic fragility differentiation within the same typological class

As already mentioned, most of the available methodologies in the literature propose the use of generic fragility curves for all bridges that fall within the same category, under the assumption that the seismic performance of bridges within the same category is similar. The validity of this assumption is investigated, based on the results of bridge-specific fragilities of all bridges within the two most frequent bridge classes of the studied road network (Fig. 5).

Table 3 – Limit state thresholds in PGA terms for all bridges of typological class #232 (longitudinal and transverse direction)

232	Fragility (Direction x)				Fragility (Direction y)				L <sub>span</sub> (m)	H <sub>pier</sub> (m)	L <sub>tot</sub> (m)	H <sub>max</sub> (m)
	LS1	LS2	LS3	LS4	LS1	LS2	LS3	LS4				
1	0.12	0.36	0.75	1.01	0.15	0.37	0.65	1.26	40	21.0÷50.60	280	50.6
2	0.13	0.37	0.75	1.50	0.13	0.38	0.74	1.68	36.3÷37.50	9.4÷26.92	335.1	26.92
3	0.11	0.28	0.53	0.90	0.11	0.23	0.65	1.45	36	11.4÷41.01	216	41.01
4	0.12	0.32	0.80	0.93	0.16	0.32	0.70	0.94	40	12.94÷38.24	200	38.24
5	0.14	0.28	0.79	1.51	0.20	0.45	0.95	1.61	36.95÷38.05	16.3÷30.27	150	30.27
6	0.15	0.40	0.89	1.44	0.22	0.45	0.89	1.78	39.1÷39.50	12.75÷30.98	157.2	30.98
7	0.15	0.45	0.89	1.41	0.18	0.38	0.75	1.45	40	12.75÷30.98	200	30.98
8	0.13	0.30	0.75	1.33	0.12	0.28	0.55	1.49	39.1÷39.50	12.75÷30.98	157.2	30.98
<b>mean</b>	<b>0.13</b>	<b>0.35</b>	<b>0.77</b>	<b>1.25</b>	<b>0.16</b>	<b>0.36</b>	<b>0.74</b>	<b>1.46</b>			<b>211.94</b>	<b>35.00</b>
<b>standard deviation</b>	<b>0.015</b>	<b>0.061</b>	<b>0.113</b>	<b>0.262</b>	<b>0.039</b>	<b>0.077</b>	<b>0.131</b>	<b>0.263</b>			<b>65.39</b>	<b>7.80</b>
<b>COV</b>	<b>11.11%</b>	<b>17.67%</b>	<b>14.66%</b>	<b>20.90%</b>	<b>24.61%</b>	<b>21.65%</b>	<b>17.84%</b>	<b>18.06%</b>			<b>30.85%</b>	<b>22.29%</b>

Table 4 – Limit state thresholds in PGA terms for all bridges of typological class #221 (longitudinal and transverse direction)

221	Fragility (Direction x)				Fragility (Direction y)				L <sub>span</sub> (m)	H <sub>pier</sub> (m)	L <sub>tot</sub> (m)	H <sub>max</sub> (m)
	LS1	LS2	LS3	LS4	LS1	LS2	LS3	LS4				
1	0.35	0.68	0.86	1.33	0.30	0.75	1.19	2.02	61.5÷112.1	41.30÷45.23	234.1	45.23
2	0.30	0.76	0.83	1.07	0.48	0.70	1.21	2.38	94.5÷160	55.00÷58.00	349	58
3	0.36	0.93	1.23	1.74	0.54	0.77	1.36	2.58	80÷120	34.20÷36.41	290	34.2
4	0.16	0.59	0.98	1.81	0.24	0.55	0.97	1.39	75.6÷120	28.12÷63.39	636.2	63.39
5	0.33	0.79	1.12	1.33	0.41	0.77	1.36	2.58	60.75÷101.5	34÷63.03	426	63.03
6	0.24	0.89	1.13	1.39	0.45	0.70	1.17	2.40	91÷144	39÷45.10	326	45.10
7	0.36	0.72	0.95	1.35	0.35	0.77	1.34	2.32	61÷107	29.12÷87.83	457	87.83
8	0.37	0.76	0.96	1.50	0.30	0.62	1.09	2.30	64.3÷118.6	35.86÷44.89	247.2	35.86
9	0.36	0.72	0.95	1.35	0.47	0.72	0.95	2.50	85	32.47	170	32.47
10	0.29	0.75	1.04	1.80	0.43	0.62	1.09	2.32	80÷86	46.08	166	46.08
11	0.41	0.65	0.82	1.42	0.42	0.75	1.29	2.05	75÷80	38.37	155	38.37
<b>mean</b>	<b>0.32</b>	<b>0.75</b>	<b>0.99</b>	<b>1.46</b>	<b>0.40</b>	<b>0.70</b>	<b>1.18</b>	<b>2.26</b>			<b>314.23</b>	<b>49.41</b>
<b>standard deviation</b>	<b>0.070</b>	<b>0.098</b>	<b>0.131</b>	<b>0.231</b>	<b>0.091</b>	<b>0.074</b>	<b>0.147</b>	<b>0.341</b>			<b>147.49</b>	<b>17.01</b>
<b>COV</b>	<b>21.97%</b>	<b>13.09%</b>	<b>13.28%</b>	<b>15.81%</b>	<b>22.81%</b>	<b>10.60%</b>	<b>12.44%</b>	<b>15.11%</b>			<b>46.94%</b>	<b>34.42%</b>

Limit state thresholds for all bridges of categories #232 and #221 (namely bridges with hollow rectangular piers connected through bearings to prestressed beam deck and monolithically connected to box-girder bridge deck, respectively) are presented in Tables 3 and 4 in PGA terms. Mean, standard deviation and coefficient of variation (COV) values based on statistical analysis of results are additionally presented, highlighting the

variation of limit state thresholds for bridges within the same category, whereas fragility curves of the generic bridge in #232 and #221 classes are depicted in Figures 11 and 12, along with upper and lower threshold values (dashed lines - range of thresholds) for each limit state.

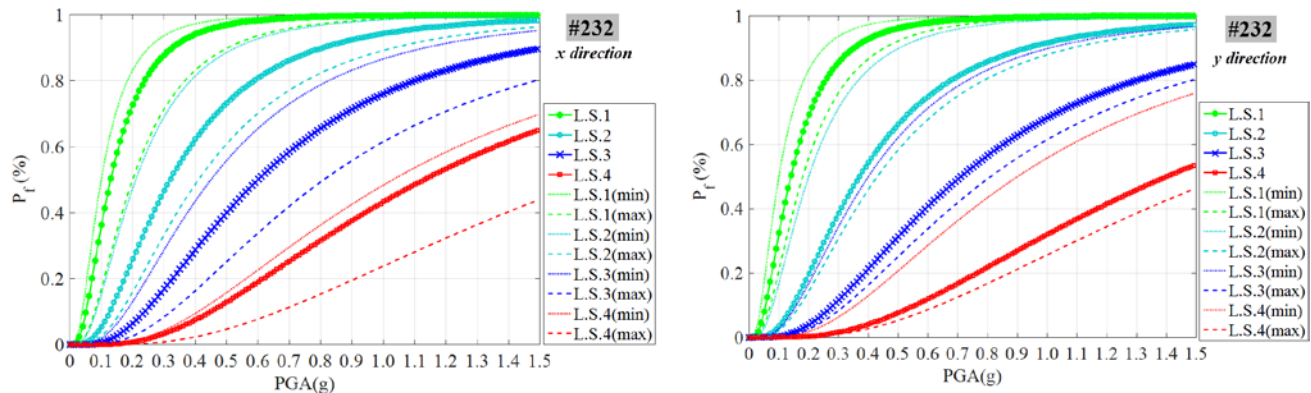


Fig. 11 – Fragility of the generic bridge in class #232 and range of damage thresholds

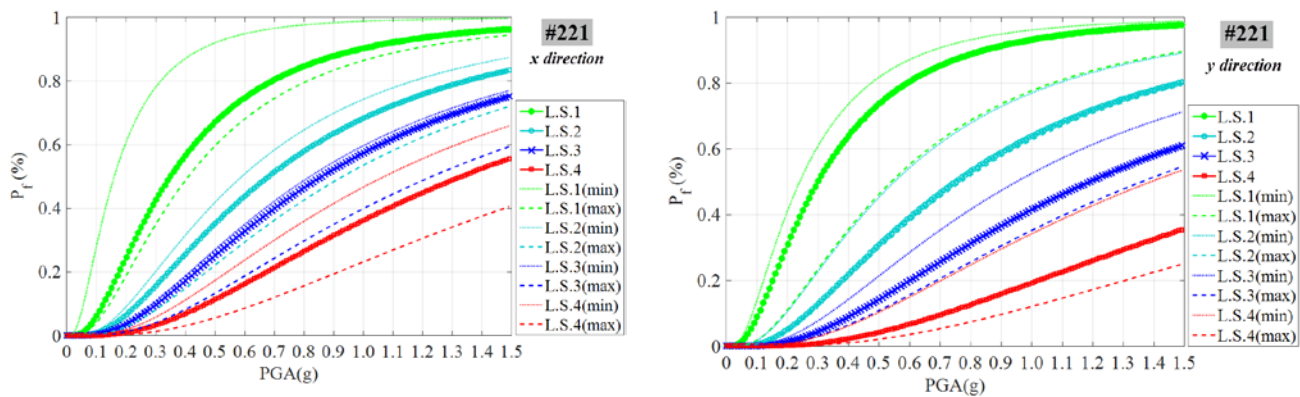


Fig. 12 – Fragility of the generic bridge in class #221 and range of damage thresholds

As far as the #232 bridge class is concerned, the variation of upper and lower level fragilities from the fragility curve of the generic bridge is small, therefore fragility curves of the bridge selected as representative can be used for all bridges that fall within the same category for the longitudinal direction and LS1 to LS3. The range of threshold values is fairly low (25% variation compared to the generic bridge) for lower limit states, however it increases for higher earthquake intensity and limit states and is dependent on the component that is critical for each limit state and the direction of loading. The variation of upper and lower level fragilities for bridge class #221 is lower for LS2 to LS4 but higher for LS1. In general, the use of the fragility curves of the generic bridge for all those in the same category may underestimate or overestimate fragility by up to 35%, however in some cases (i.e. LS1 for bridge class #221 and LS4 for #221) the underestimation may reach 50%.

### 3.4 Effect of pier height and total bridge length on bridge fragility

The effect of pier height(s) and total bridge length on bridge fragility (LS4 damage thresholds) is depicted in Figures 13 to 15 for all bridges of the inventory. The variation of threshold values is obvious, highlighting the effect of bridge geometry (i.e. pier height and total length) on seismic fragility and the importance of bridge-specific fragility curves in the seismic assessment of a road network. In Fig.13, the variation of limit state threshold values in PGA terms with varying maximum pier height is presented. Since the range of pier heights and the number of piers are not accounted for, an equivalent height ( $H_{equiv}$ ) is proposed (Eq. (2), Fig.14), considering the heights of all piers ( $h_i$ ) and the number of piers ( $n$ ), in order to evaluate the effect of pier height on system fragility; clearly this is a simplified way to address the issue, not appropriate for extreme cases, such as the presence of a short pier in the middle of the bridge (found in some poorly designed existing bridges).

$$n \cdot \frac{1}{h_{eq}^3} = \sum_i^n \frac{1}{h_i^3} \quad (2)$$

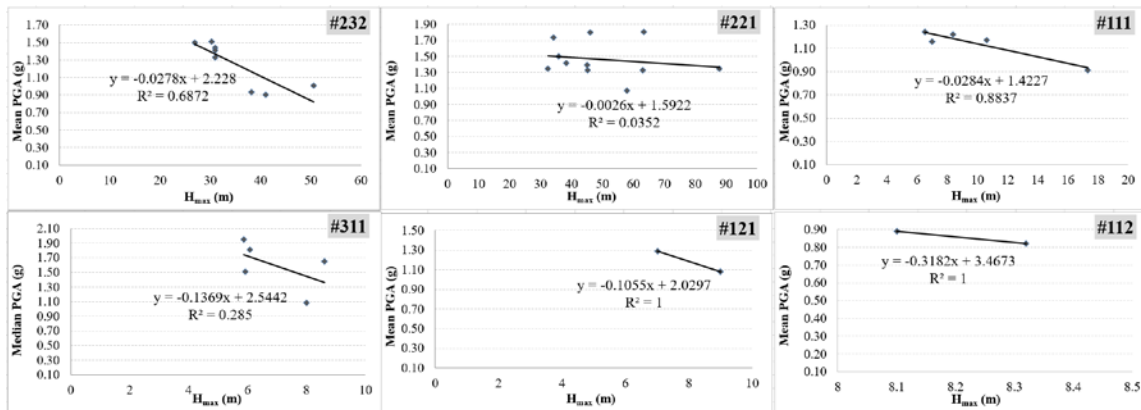


Fig. 13 – Effect of maximum pier height on seismic fragility of different bridge classes

As seen in Fig. 14, bridges having shorter piers (lower  $h_{eq}$ ) are in general more vulnerable, however it should be highlighted that the threshold values refer to the bridge system rather than the individual components. The general trend and the relevant limit state threshold value variation is depicted in Fig.14 for different bridge classes and limit states (piers are the most critical components for the cases shown).

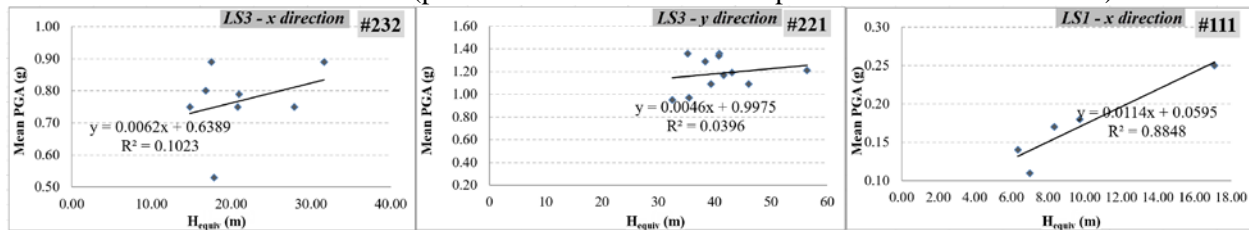


Fig. 14 – Effect of equivalent pier height on seismic fragility of different bridge classes

Finally, based on Fig. 15, it appears that the effect of total length on bridge system fragility varies, depending on the bridge class and structural system; no clear trends can be identified in this case.

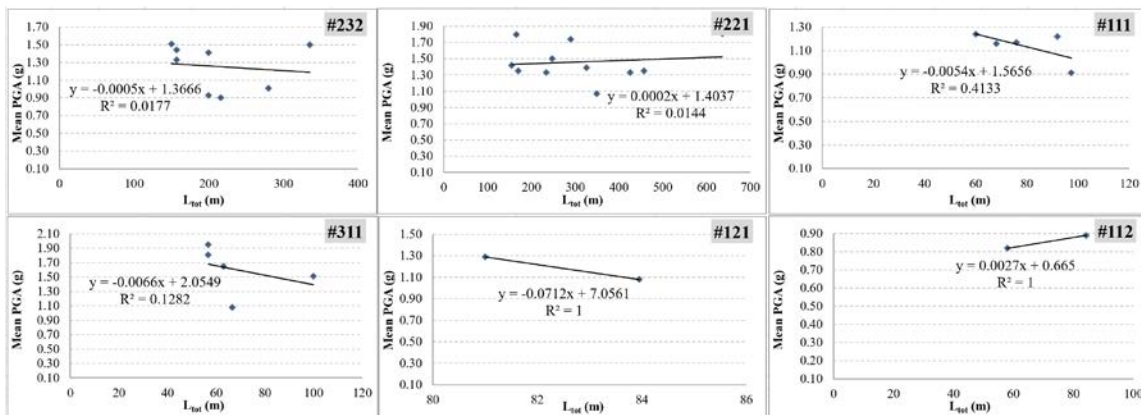


Fig. 15 – Effect of total bridge length on seismic fragility of different bridge classes

#### 4. Conclusions

The most important findings from the application of the proposed component-based methodology to a specific bridge stock (in Southern Europe) are summarised in the following.

- Pier type has an important effect on system fragility for the case of bridges with box-girder decks and monolithic pier-to-deck connection, since piers are the most critical component for this bridge type. The effect of pier type on the fragility of simply-supported (through elastomeric bearings) bridges is lower, since the bearings are the most critical component for this bridge class for the majority of limit states considered.
- Bridges with single-column cylindrical piers monolithically connected to slab or box-girder decks are more vulnerable than similar bridges having multi-column cylindrical, wall or hollow rectangular piers. Among

bridges with monolithic pier-to-deck connection, bridge class #221, i.e. bridges with hollow rectangular piers monolithically connected to box-girder deck are the less vulnerable class (transverse direction).

- The effect of different deck type, namely slab or box girder, on bridge fragility of bridges having single column cylindrical piers connected to the deck through elastomeric bearings (classes #122 and #112), is in general minor.
- Regarding the effect of pier-to-deck connection on bridge fragility, monolithic bridges are less vulnerable for all limit states and both the longitudinal and transverse direction compared to simply-supported bridges; different components are critical in each case (piers and bearings, respectively).
- The use of generic bridge fragility curves for all bridges belonging to the same category may underestimate or overestimate fragility, typically by up to 35%, however in some cases the underestimation may reach 50%, which is clearly an issue of concern. The range of LS threshold values is fairly narrow for lower limit states, but it increases for higher earthquake intensity and higher limit states (heavy damage, failure).
- The variation of threshold limit state values for bridges of the same category with varying pier heights and total length, highlights the need for bridge-specific fragility curve development.

## 5. Acknowledgements

This research has been co-financed by the European Union (European Social Fund – ESF) and Greek national funds through the Operational Programme “Education and Lifelong Learning” of the National Strategic Reference Framework (NSRF) – Research Funding Program: *ARISTEIA II: Reinforcement of the interdisciplinary and/or interinstitutional research and innovation*.

## 5. References

- [1] Avşar Ö, Yakut A, Caner A (2011): Analytical Fragility Curves for Ordinary Highway Bridges in Turkey. *Earthquake Spectra*, **27** (4), 971–996.
- [2] Elnashai, A. S., Borzi, B., & Vlachos, S (2004): Deformation-based vulnerability functions for RC bridges. *Structural Engineering and Mechanics*, **17**(2), 215–244.
- [3] Moschonas I F, Kappos A J, Panetsos P, Papadopoulos V, Makarios T, Thanopoulos P (2008): Seismic fragility curves for greek bridges: methodology and case studies. *Bulletin of Earthquake Engineering*, **7**(2), 439–468.
- [4] Shinozuka M, Feng M Q, Lee J, Naganuma T (2000): Statistical Analysis of Fragility Curves. *Journal of Engineering Mechanics*, ASCE, **126**(12), 1224–1231.
- [5] Mander J, Basöz N (1999): *Enhancement of the Highway Transportation Lifeline Module in HAZUS*. Final Pre-Publication Draft (#7) prepared for National Institute of Building Sciences (NIBS).
- [6] Tsionis G, Fardis MN (2012): Seismic Fragility of Concrete Bridges with Deck Monolithically Connected to the Piers or Supported on Elastomeric Bearings. *15th World Conference of Earthquake Engineering*. Lisbon, Portugal.
- [7] DesRoches R, Padgett J, Ramanathan K, Dukes J (2012): Feasibility Studies for Improving Caltrans Bridge Fragility Relationships. *Technical Report CA12-1775*, Georgia Institute of Technology, Atlanta, U.S.A.
- [8] Tavares D H, Padgett JE, Paultre P (2012): Fragility curves of typical as-built highway bridges in eastern Canada. *Engineering Structures*, **40**, 107–118.
- [9] Stefanidou SP, Kappos AJ (2015): Methodology for the Development of Structure- Specific Fragility Curves for Bridges in a Road Network. *5<sup>th</sup> International Conference on Computational Methods in Structural Dynamics and Earthquake Engineering, COMPDYN 2015*, Crete Island, Greece.
- [10] Stefanidou SP (2016): *Structure-specific Fragility Curves for As-Built and Retrofitted Bridges*. PhD Thesis (In Greek), Aristotle University of Thessaloniki.
- [11] McKeena F, Fenves GL (2015): *Open System for Earthquake Engineering Simulation*. Pacific Earthquake Engineering Research Center, Version 2.4.5.